Structural, Electrical and Dielectric Behavior of
Ni$_x$Co$_{1-x}$Pr$_y$Fe$_{2-y}$O$_4$ Nano-Ferrites Synthesized by Sol-Gel Method

[1]Muhammad Tahir Farid*, [1]Ishtiaq Ahmad, [1]Ghulam Murtaza [1]Irshad Ali and [2]Imtiaz Ahmad
Department of Physics, Bahauddin Zakariya, University Multan, 60800. Pakistan.
Institute of Chemical Sciences, Bahauddin Zakariya, University Multan, 60800. Pakistan.
tahir95263@yahoo.com*

Summary: The influence of praseodymium (Pr) contents on the structural, electrical and dielectric properties of Ni$_x$CO$_{1-x}$Pr$_y$Fe$_{2-y}$O$_4$ ferrites was investigated. This series was prepared by sol-gel method. XRD analysis reveals single phase samples up to y ≤ 0.04. At y ≥ 0.06, a secondary phase of iron praseodymium oxide (PrFeO$_3$) appears along with the spinel phase. The incorporation of Pr^{3+} for Fe^{3+} ions results in a slight increase of lattice constant due to larger ionic radius of the substituted ions. It was inferred that the substitution of praseodymium limits the grain growth. The DC electrical resistivity and activation energy are higher for the substituted samples. The dielectric constant, dielectric loss (tan δ) and AC-conductivity decreased on account of substitution. The decrease in dielectric constant is imputed to the reduction in the internal viscosity of the substituted samples. Ferrites have high dielectric constant and low tan δ, they may be attractive for application in switching and memory storage devices.

Key words: Solgel method, Pr, Cubic spinel Ferrites, DC resistivity, Drift mobility, Dielectric properties.

Introduction

Ferrite materials have been widely used to prepare many electromagnetic devices such as inductors, converters, phase shifters and electromagnetic wave absorbers [1]. The fabrication of spinel ferrites nanoparticles has been the subject of intense research interest due to their excellent magnetic, electrical and dielectric properties [2]. The ferrites behave as inhomogeneous dielectric materials in which individual high-conducting grains are separated by either air gaps or low-conducting layers. Due to high resistivity, low eddy current losses and convincingly low costs coupled with their potential microwave applications such as circulators, isolators and phase shifters, lithium ferrites have fascinated considerable interest for many researchers [3]. Cobalt ferrite has a partially inverse spinel structure in which both sites, i.e. tetrahedral (A) and octahedral (B) sites, contain a fraction of Co^{2+} and Fe^{3+} cations; however it is generally accepted that a large fraction of Co^{2+} ions are on the B-site and the remaining are on the A-site, which depends on the production methods as well as on the heat treatment procedure [4–6]. Rare earth ions have unpaired 4f electrons. The fourth shell ions are shielded by the ions in the fifth shell and are hardly affected by the potential field of the surrounding ions [7]. By introducing rare earth ions into the system, the Pr^{3+}–Fe^{3+} interactions appear (3d–4f coupling) which affect the electrical and magnetic properties of the spinel ferrites. Substitution of rare earth ions into the spinel structure lead to structural distortion which modify the electrical transport properties. Studies concerning the effects of substitution of Tb, Dy, Yb, Er, Gd, Sm, Ce, Y, Eu, La, Th, etc., in various spinel ferrites have been carried out by several researchers [8–10]. Incorporation of various substitutions and different molar ratios in Ni–Co ferrite was studied [11, 12]. Substitution of rare earth ion into the spinel structure shows structural distortion [13–15] inducing strain in the sample with significant change in the electrical and magnetic properties. The structural, dielectric and transport properties of rare earth doped Ni ferrite were reported by Dwevedi *et al*. [16].

Earlier Investigators have focused their attentions for modification of the inherent magnetic and electrical properties of ferrites by substituting with either single trivalent metal ions like Cr, La, Nd [17]or the suitable combination of divalent + trivalent, Co–La [18]or combination of divalent + tetravalent ions, Ni–Zr [19]. Narang *et al*. [20] reported the microwave dielectric properties of Co–Ti doped M-type hexaferrite. Iqbal *et al*. [21] reported the effect of Ce–Ni substitution on the electrical and magnetic properties of Sr–Ba M-hexaferrite. Singh *et al*. [22] studied the magnetic properties of Co–Ru substituted Sr– Ba hexaferrite. Iqbal *et al*. [23] reported the Nanometer-sized crystallites of Y-type strontium hexaferrite, Sr$_2$Ni$_2$Fe$_{12}$O$_{22}$ and its Mn- and Cr-doped derivatives. Ashiq *et al*. [24] adopted the solgel method to synthesize the Er-Ni substituted M-type hexaferrites. Asghar *et al*. [25] investigated structural, dielectric and magnetic properties of Cr-Zn doped strontium

---

hexa-ferrites for high frequency applications. Sadiq *et al.* [26], studied the influence of Nd-Co Substitution on structural, electrical, and dielectric properties of X-Type hexagonal nanoferrites.

However, the cobalt doping of rare-earth elements along with the combination of transition metals is seldom reported in spinel ferrites. In this study, we synthesized Ni^{2+} and Pr^{3+} substituted derivatives of in spinel ferrites materials by using the Sol-Gel method to investigate the effect of substitution of Ni^{2+} and Pr^{3+} at octahedral site in order to observe changes in electrical properties, such as, Dc resistivity, drift mobility, dielectric constant and dielectric loss. As a part of search for new material with novel properties. In the latter context, the demand for microwave properties invoked the current interest in fabricating the fine particles of substituted spinel ferrite low value of dielectric constant. The purpose of the investigation is to study the effect of Praseodymium ions substitution for nickel cobalt ions on structural, electrical and dielectric properties of $Ni_xCO_{1-x}Pr_yFe_{2-y}O_4$ ferrites to make these ferrites suitable for switching and memory storage devices applications.

Experimental

$Ni_xCO_{1-x}Pr_yFe_{2-y}O_4$ (x= 0.00, 0.20, 0.40, 0.60, 0.80, 1.0 and y = 0.00, 0.02, 0.04, 0.06, 0.08, 0.1) nano ferrites were synthesized by sol–gel auto-combustion technique. Analytical grade Co $(NO_3)_2$, Ni $(NO3)_2$, Fe_3Cl_2 and Pr_2O_3 (99.99% pure) were dissolved initially in 100 ml de-ionized water in a Pyrex beaker. To obtain homogenous and transparent solution, citric acid was used as a chelating agent. Dissolved solution was mixed homogeneously by placing it on magnetic stirrer at the temperature of 80 °C . pH value was maintained at 7–8 by adding ammonia solution continuously followed by stirring for 6–7 hours. The solution transformed into viscous gel first and then a self-combustion phenomenon occurred at temperature 370 °C. Dry gel converted into fluffy powder called ''precursor powder'' after its complete burning. The powder, after complete grinding, was then pre-sintered at 700 °C in a furnace for 5 hours, followed by furnace cooling. These sintered powders were then pressed into pellets under the load of (~30 KN) by using Paul–Otto Weber Hydraulic Press. The pellets were formed using (3–5 wt %) polyvinyl alcohol as a binder. The binder was evaporated at 250 °C for 1 hour and finally samples were sintered again at 950 °C for 7 hours.

The structural characterization of all the samples was carried out by the X-ray diffraction. XRD data were taken at room temperature using $CuK_α$ (λ = 1.5406A°) radiation. dc electrical resistivity for all these samples was measured by two-probe method. The electrical resistivity was measured with sample pellet of 2.0 mm thickness and 13mm diameter. For dielectric measurements silver paint was applied on both sides of the pellets and air dried to have good ohmic contact. The dielectric measurements were made using a precision LCR meter (Wayne Kerr LCR 4275) at room temperature in the frequency range 1 MHz to 3 GHz. Using LCR meter the dielectric parameters such as Capacitance of the pellet, tan δ (loss tangent) and Capacitance of air with the same thickness as the pellet were measured. The real part of dielectric constant ($ε'$) was determined from the following formula.

$$\varepsilon' = \frac{C_p}{C_{Air}} \tag{1}$$

Where:

$ε'$ = Real part of dielectric constant
C_p = Capacitance of the Pellet in Faraday
C_{Air} = Capacitance of Air in Faraday

The imaginary part of the dielectric constant ($ε''$) or dielectric loss was measured by using the following relation.

$$\varepsilon'' = \varepsilon' \tan\delta \tag{2}$$

$ε'$ = Real part of dielectric constant
tan δ = loss tangent

Results and Discussion

X-Ray Studies

X-ray diffraction patterns of $Ni_xCO_{1-x}Pr_yFe_{2-y}O_4$ (x= 0.00, 0.20, 0.40, 0.60, 0.80, 1.0 and y = 0.00, 0.02, 0.04, 0.06, 0.08, 0.1) ferrite system are shown in Fig. 1.

All the samples show good crystallization, with well-defined diffraction peaks. Table-1 shows the composition of the phases precipitated and the lattice constants of the $Ni_xCO_{1-x}Pr_yFe_{2-y}O_4$ ferrites. For y ≤ 0.04, the samples have the monophase cubic spinel structure while for y ≥0.06, the samples are biphasic. The presence of the strong diffraction peaks corresponding to the planes (111), (220), (311), (222), (400), (422), (511/333), (440) indicates the presence of cubic spinel phase. Miller indices (h k l)

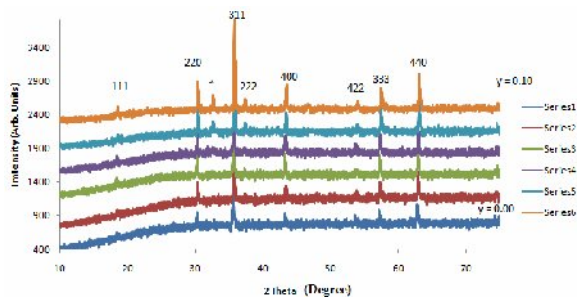and inter-planer spacing (d) for $Ni_xCO_{1-x}Pr_yFe_{2-y}O_4$ ferrites system are listed in Table-1.

Fig. 1:   X-Ray D iffraction patterns of $Ni_xCO_{1-x}Pr_yFe_{2-y}O_4$ ferrites.

A peak corresponding to $2\Theta=33.1°$ (indicated by * in Fig. 1) is attributed to secondary phase at the grain boundaries and appears for $y \geq 0.06$ and magnitude of intensity increases with the increase of Praseodymium concentration. This peak is identified as $FePrO_3$ (iron praseodymium oxide) matched with ICDD PDF # 39-1489. The secondary phase on the grain boundaries appears due to high reactivity of Fe^{3+} ions with Pr^{3+} ions [27]. The lattice constant (a) increases slightly for all the compositions are shown in Fig. 2.
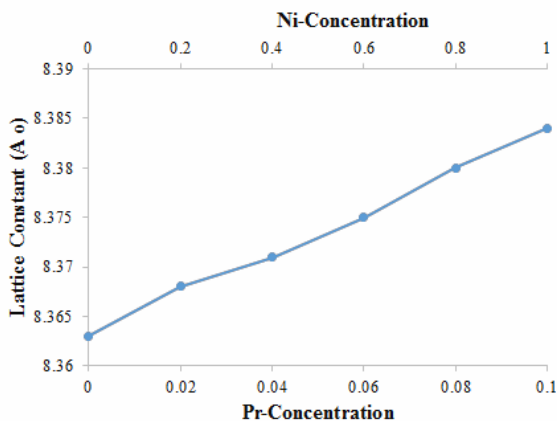

Fig. 2:   Lattice Constant 'a' of $Ni_xCO_{1-x}Pr_yFe_{2-y}O_4$ ferrites.

The variation can be explained on the basis of ionic radii of the substituted ions. The replacement of the smaller Fe^{3+} ions (0.64 °A) with larger Pr^{3+} ions (1.013° A) causes dilation of the host spinel lattice which results in the increase of lattice constant. This observation is consistent with the results reported by various authors where it has been reported that the substitution of rare earth ions increases the lattice constant [28, 29, 30]. The lattice parameter for biphasic samples still increases with Praseodymium

contents which enables us to conclude that the spinel lattice is not compressed by the secondary phase. Thus, there is no solubility limit for Praseodymium ions (rare-earth transition metal) in this ferrite in the given range ($y \geq 0.12$). Such observation in the lattice constant in rare-earth substituted ferrites has been reported by Hemeda *et al.* [31] in case of $NiGd_xFe_{2-x}O_4$. The measured particle size of all the samples by Scherrer's formula [32] is given in Table-1.

$$D = \frac{0.9\lambda}{\beta \cos \theta} \qquad (3)$$

Where β is the full width half maximum (rad), λ the wavelength of the X-ray, Θ is the angle between the incident and diffracted beams (degree) and D the particle size of the sample (nm). This confirms that the citric acid is more effective burning agent for producing fine ferrite powder with sol–gel auto combustion method. Homogeneity of the chemical composition of the ferrite particles was acquired by thermal decomposition of nitrates.

Table-1:Phases, X-ray density, Bulk Density and grain size of $Ni_xCO_{1-x}Pr_yFe_{2-y}O_4$ ferrites.

Composition		Secondary Phase	X-ray Density (g/cm³)	Bulk Density (g/cm³)	Grain Size (nm)
x	y				
0.00	0.00	-----	5.376	4.18	28.48
0.20	0.02	-----	5.423	4.26	37.36
0.40	0.04	-----	5.457	4.35	46.80
0.60	0.06	PrFeO₃	5.489	4.38	53.30
0.80	0.08	PrFeO₃	5.524	4.41	58.86
1.00	0.10	PrFeO₃	5.571	4.43	63.03

The X-ray density was calculated by using the following equation [33, 34]:

$$D_x = 8M/N_Aa^3 \qquad (4a)$$

where M is the molar mass of the ferrite, a is the lattice parameter, and N_A is Avogadro's number.

Sintered density was calculated from the measured mass and volume of the pellets. Mass was measured using digital balance and volume was calculated from external dimensions of the pellets. The bulk density "D" was also determined by using Archimedes principles in toluene as:

$$D = \frac{wt\,of\,sample\,in\,air}{wt\,of\,sample\,in\,air\,-\,wt\,of\,sample\,in\,toluene} \times density\,of\,toluene \qquad (4b)$$

where density of the toluene is 0.857 g/cm³.

The dependence of D_x and D on Pr-concentration y is presented in Table-1. It can be

observed from these tables that bulk densities are smaller in magnitude than corresponding X-ray densities.

X-Ray density (D_x) increase linearly with increase in Pr concentration, from 5.33 g/cm^3 to 6.08 g/cm^3. Also the bulk density (D) increases from 4.18 g/cm^3 to 4.43 g/cm^3. The increase in D_x and D with increase in Pr concentration may be attributed to the replacement of Fe^{3+} ions by larger mass of Pr^{3+} ions.

Electrical Properties

Room temperature dc resistivity measured by two probe method as a function of Pr-concentration are reported in Fig. 3 which clearly demonstrating the increasing trend of resistivity with increase in Pr and Ni concentration.
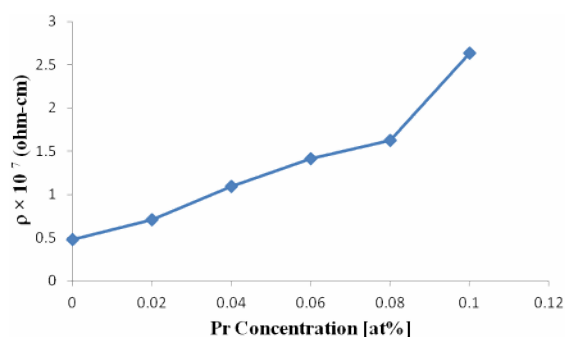

Fig. 3:   The log of room temperature dc resistivity as a function of Pr-Concentration y

In $Ni_xCO_{1-x}Pr_yFe_{2-y}O_4$ (x= 0.00, 0.20, 0.40, 0.60, 0.80, 1.0 , y = 0.00, 0.02, 0.04, 0.06, 0.08, 0.1) alloys, the concentration of Fe^{3+} ions on Octahedral sites gradually decreases with increasing y while the substituted Pr^{3+} partially occupies the corresponding empty location. As the Pr^{3+} ions has large ionic radius which may be one of the causes to decrease the hopping rate of electron as it enhances the separation between Fe^{2+} and Fe^{3+} ions and consequently, enhances the dc resistivity and activation energy. These results are consistent with the results reported by various authors [35, 36]. Similar results with Dy doping in Ni-Co ferrites has been reported by [37]. The temperature dependent dc resistivity measured using two probe method in the temperature range 303 -573 K for $Ni_xCO_{1-x}Pr_yFe_{2-y}O_4$ (x= 0.00, 0.20, 0.40, 0.60, 0.80, 1.0 , y = 0.00, 0.02, 0.04, 0.06, 0.08, 0.1), as a function of temperature are given in Fig. 4 .

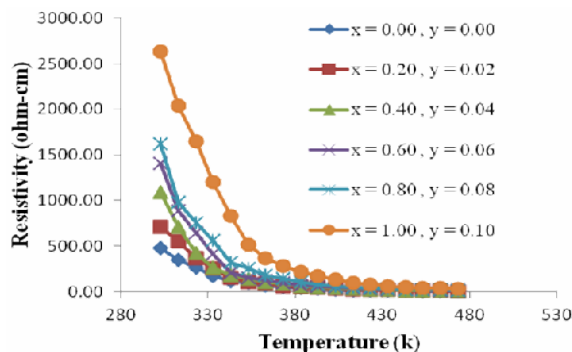Fig. 4:   The dc resistivity as a function of temperature for $Ni_xCO_{1-x}Pr_yFe_{2-y}O_4$ ferrites.

These graphs show that the increase in temperature leads to decrease in resistivity which is the normal behavior of semiconducting materials and it obeys the well known Arrhenius relation [38]. The higher values of temperature for the samples help the trapped charges to be librated and participate in the conduction process which results decrease in resistivity. Conductivity of spinel ferrites vs Temperature (k) is shown in fig 5 (a). According to the conduction mechanism in ferrites, the decrease in resistivity could also be related to the increase in the drift mobility of the thermally activated electrons [39, 40].

Drift mobility (μ_d) is calculated from electrical resistivity data using the following relation [41–43]:

$$\mu_d = \frac{1}{ne\rho} \tag{5}$$

where e is the charge of electron, ρ is electrical resistivity and n is the concentration of charge carriers and can be calculated using following equation:

$$n = \frac{N_A C_{Fe} \rho_b}{M} \tag{6}$$

where N_A is the Avogadro's number, C_{Fe} the number of iron atoms in the chemical formula of the samples, ρ_b the bulk density and M is the molar mass of the samples. Fig. 5(b) shows the variation of drift mobility with temperature.

It is observed that the drift mobility increases with the increase in temperature. This is due to the fact that the charge carriers start hopping from one site to another as the temperature increases.

Dielectric Properties

Compositional Effect on Electrical Permittivity

The variation of dielectric constant and complex dielectric constant determined vs Pr concentration for $Ni_xCO_{1-x}Pr_yFe_{2-y}O_4$ (x= 0.00, 0.20, 0.40, 0.60, 0.80, 1.0 and y = 0.00, 0.02, 0.04, 0.06, 0.08, 0.1) ferrites at room temperature are shown in Figs. 6 and 7 respectively.
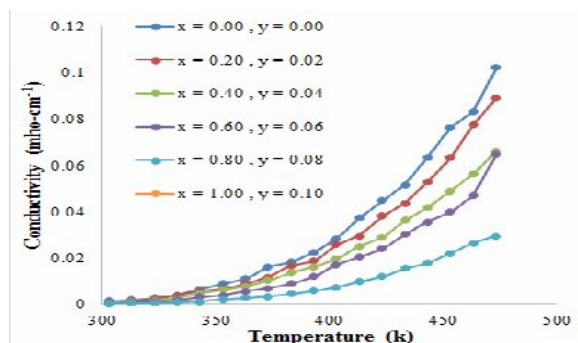

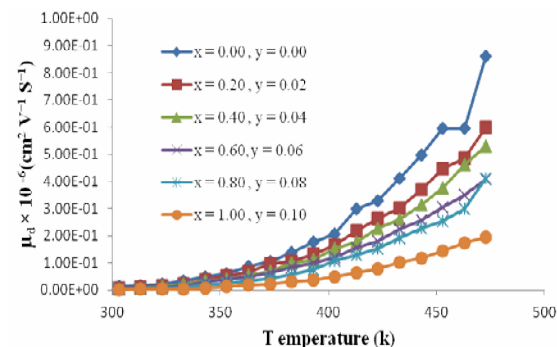Fig. 5(a): Conductivity as a function of temperature for $Ni_xCO_{1-x}Pr_yFe_{2-y}O_4$ ferrites.

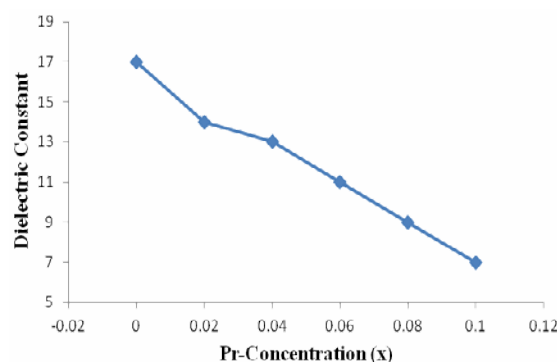Fig. 5(b): Drift mobility as a function of temperature for $Ni_xCO_{1-x}Pr_yFe_{2-y}O_4$ ferrites.

Fig. 6: Dielectric constant vs Pr-concentration (x) for $Ni_xCO_{1-x}Pr_yFe_{2-y}O_4$ ferrites.

It can be seen from the Fig 6 and 7 that both ε' and ε'' decrease with the increase of Praseodymium concentration. It was observed that the electronic exchange between Fe^{2+} and Fe^{3+} results in local displacements, determining the polarization of charges in these ferrites. Thus, it is the number of ferrous ions on octahedral sites that play a dominant role in the process of conduction and dielectric polarization. Due to larger ionic radius, Pr^{3+} ions occupy octahedral sites [44]. The concentration of Fe^{3+} ions at B-sites decreases gradually with increasing concentration of Praseodymium up to y = 0.02. At y> 0.02, the reduction in the values of dielectric constant and complex dielectric constant with increasing concentration of Praseodymium is due to depicting concentration of iron ions at B-sites which play a dominant role in dielectric polarization due to the presence of second phase. The electron transfer between Fe^{2+} and Fe^{3+} ions will be hindered i.e. the polarization decreases. Consequently, both dielectric (ε') and complex dielectric constant (ε'') decrease with Praseodymium contents[45].
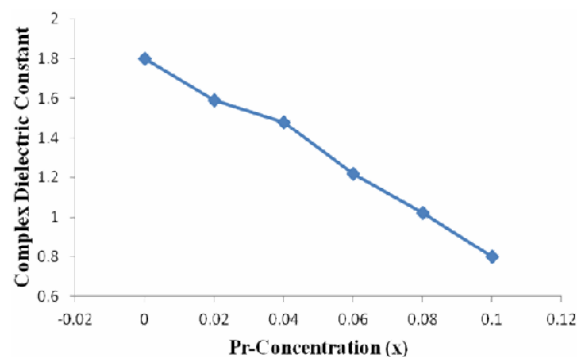

Fig. 7: Complex Dielectric constant vs Pr-concentration (y) for $Ni_xCO_{1-x}Pr_yFe_{2-y}O_4$ ferrites.

Effect of Frequency on Dielectric and Complex Dielectric Constant

At room temperature, the real and imaginary part of dielectric constant (ε' and ε'') of $Ni_xCO_{1-x}Pr_yFe_{2-y}O_4$(x= 0.00, 0.20, 0.40, 0.60, 0.80, 1.0, y = 0.00, 0.02, 0.04, 0.06, 0.08, 0.1) as a function of frequency in the range of 1 MHz to 3GHz were studied and results had been plotted in Fig. 8 and 9.

At high frequency, the values of ε' and ε'' are almost constant. Similar results were observed by [46]. From graphs, it is clear that all the samples have higher dielectric constant at lower frequency. The decrease in ε' is sharp initially at lower frequency and then ε' value decreases slowly with the increase in frequency and showed almost frequency independent behavior at high frequency regions, similar behavior

was observed by [47]. The variation of dielectric constant with frequency may be explained on the basis of space-charge polarization phenomenon [48]. According to space-charge polarization phenomenon, dielectric material has well conducting grains, which are separated with highly resistive grain boundaries. When electric field is applied, space charge accumulates at the grain boundaries and voltage drops mainly at grain boundaries. Koops proposed that grain boundary effect is more at low frequencies [49]. When the frequency given to dielectric material is increased beyond a specific limit the electron exchange between Fe^{2+} and Fe^{3+} ions does not follow the variations of applied field, and the value of dielectric constant almost becomes constant. According to Maxwell and Wagner two layer model, the dielectric structure of ferrite material is assumed to be made of two layers [50]. First layer is a conducting layer, which consist of large conducting ferrite grains separated by other thin weakly conducting intermediate grain boundaries. [51] Pointed out that polarization in ferrites is through a mechanism, which is similar to the conduction process. The exchange of electron between ferrous and ferric ions, results in local displacement of electrons in the direction of field that is applied to the dielectric material determines polarization. As the frequency increases, the Polarization decreases and then approaches a constant value. The fact behind that behavior is that, when applied field increases a specific frequency of external field, the electron exchange $Fe^{2+}\leftrightarrow Fe^{3+}$ cannot follow the alternating field. The high value of dielectric constant at lower frequency is due to the predominance of the species like Fe^{2+} ions, oxygen vacancies, grain boundary defects, etc while the decrease in dielectric constant with frequency is natural that is any species contributing to the polarizability is found to show the applied field lagging behind at higher frequencies[52].
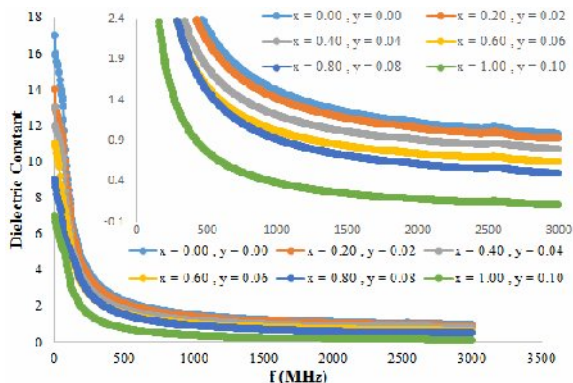

Fig. 8:　Dielectric constant vs frequency (MHz) for $Ni_xCO_{1-x}Pr_yFe_{2-y}O_4$ ferrites.

Loss Tangent (tan δ)

The loss tangent is a parameter of a dielectric material that quantifies its inherent dissipation of electromagnetic energy at different frequencies. It measures the loss of electrical energy from the applied electric field into the samples at different frequencies.
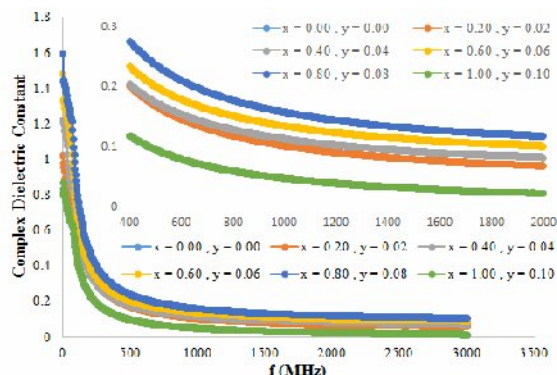

Fig. 9:　Complex Dielectric constant vs frequency (MHz) for $Ni_xCO_{1-x}Pr_yFe_{2-y}O_4$ ferrites.

Fig. 10 shows that the loss decreases rapidly in the low frequency region while the rate of decrease is slow in high-frequency region and it shows an almost frequency independent behavior in high frequency region. The behavior can be explained on the basis that in the low frequency region, which corresponds to a high resistivity (due to the grain boundary), more energy is required for electron exchange between Fe^{2+} and Fe^{3+} ions, as a result the loss is high. In the high frequency region, which corresponds to a low resistivity (due to the grains), small energy is required for electron transfer between the two Fe ions at the octahedral site. Moreover, the dielectric loss factor also depends on a number of factors such as stoichiometry, Fe^{2+} content, and structural homogeneity which in turn depend upon the composition and sintering temperature of the samples [53]. Also it is known that there is strong correlation, between the conduction mechanism and the dielectric constant behavior (Polarization mechanism) in ferrites. At high frequencies the peaking behavior is observe. This type of peaking behavior (Debye-type relaxation) is observed when the jumping frequency of the Fe^{+2} and Fe^{+3} ions is exactly equal to the frequency of the applied field [48] i.e.

$$\omega\tau = 1 \tag{7}$$

where τ is the relaxation time of hopping process and ω is the angular frequency of the field. This shows

that with increase in Pr concentration the energy losses decrease at high frequencies. The low loss values at higher frequencies show the potential applications of these materials in high frequency micro wave devices.
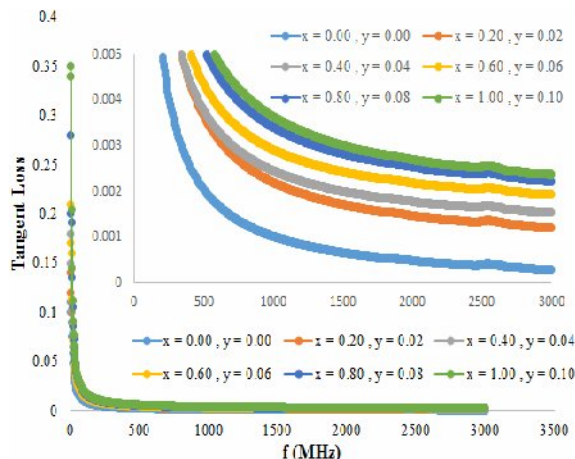

Fig. 10: Tangent loss vs frequency (MHz) for $Ni_xCO_{1-x}Pr_yFe_{2-y}O_4$ ferrites.

Conclusions

Structure, electric and dielectric properties of different composition prepared by sol-gel method has been investigated and results discussed systematically. X-ray diffraction analysis reveals that $Ni_xCO_{1-x}Pr_yFe_{2-y}O_4$ (x= 0.00, 0.20, 0.40, 0.60, 0.80, 1.0 and y = 0.00, 0.02, 0.04, 0.06, 0.08, 0.1) samples clearly indicate formation of cubic spinel crystal structure and secondary phase is also identified in last three samples. Lattice constant exhibits increase from 8.363 A^o to 8.384 A^o as a function of Pr concentration (y). X-ray density and bulk density have increasing trend with substitution of host elements. Room temperature dc resistivity of $Ni_xCO_{1-x}Pr_yFe_{2-y}O_4$ ferrites increases with increase in praseodymium concentration. This was attributed to the formation of insulating intergranular layers that impedes the oxidation of Fe^{2+} ions inside the grains. Temperature dependent dc electrical resistivity decreases as the temperature increases which is indicating semi-conductor behavior of the samples. It was concluded that samples having low resistivity have low activation energy and vice versa. High value of dc resistivity makes this ferrite suitable for the high frequency applications where eddy current losses become appreciable. Calculated drift mobility increases with increase in temperature. The dielectric constant and dielectric loss attain very low values at higher frequency for higher concentration of praseodymium ions. The values of dielectric constant for y = 0.00 are much greater than those of y = 0.10

which is the direct effect of praseodymium ions substitution. Low values of dielectric constant and dielectric losses exhibited by this ferrite suggest its utility in microwave communications.

References

1. V. G. Harris, A. Geiler, Y. J. Chen, S. D. Yoon, M. Z. Wu, A. Yang, Z. H. Chen, P. He, P. V. Parimi, X. Zuo, C. E. Patton, M. Abe, O. Acher and C. Vittoria, Recent Advances in Processing and Applications of Microwave Ferrites, *J. Magn. Magn. Mater.,* **321**, 2035 (2009).
2. Y. P. Fu, S. H. Hu, Electrical and Magnetic Properties of Magnesium-Substituted Lithium Ferrite, *Ceram. Int.,* **36**, 1311 (2010).
3. Yen-Pei Fua, Dung-Shing Hung, Yeong-Der Yao, Microwave Properties of Chromium-Substituted Lithium Ferrite, *Ceram. Int.,* **35**, 2179 (2009).
4. Md. T. Rahman, C. V. Ramana, Gadolinium-Substitution Induced Effects on the Structure and AC Electrical Properties of Cobalt Ferrite, *Ceram. Int.,* **40**, 14533 (2014).
5. R. W. McCallum, K. W. Dennis, D. C. Jiles, J. E. Snyder, Y. H. Chen, Composite Magnetostrictive Materials for Advanced Automotive Magnetomechanical Sensors, *Low Temperature Physics*, **27**, 266 (2001).
6. Y. Chen, J. E. Snyder, C. R. Schwichtenberg, K. W. Dennis, R. W. McCallum, D. C. Jiles, Metal-bonded Co-Ferrite Composites for Magnetostrictive Torque Sensor Applications, *IEEE Transactions on Magnetics* , **35**, 3654 (1999).
7. T. J. Shinde, A. B. Gadkari, P. N. Vasambekar, Effect of Nd3+ Substitution on Structural and Electrical Properties of Nanocrystalline Zinc Ferrite, *J. Magn. Magn. Mater.,* **322**, 2777 (2010).
8. M. A. Khan, M. U. Islam, M. Ishaque, I. Z. Rahman, Effect of Tb Substitution on Structural, Magnetic and Electrical Properties of Magnesium Ferrites, *Ceram. Int.,* **37**, 2519 (2011).
9. E. Rezlescu, N. Rezlescu, P. D. Popa, L. Rezlescu, C. Pasnicu, The Influence of R_2O_3 (R = Yb, Er, Dy, Tb, Gd, Sm and Ce) on the Electric and Mechanical Properties of a Nickel–Zinc Ferrite, *Phys. Stat. Sol.* (a)., **162**, 673 (1997).
10. M. A. Ahmed, N. Okasha, M. M. El-Sayed, Enhancement of the Physical Properties of Rare-Earth-Substituted Mn–Zn Ferrites Prepared by Flash Method*, Ceram. Int.,* **33**, 49 (2007).

11. K. K. Patankar, S. S.Joshi, B. K. Chougule, Dielectric Behaviour in Magnetoelectric Composites, *Physics Letters* A, **346**, 337 (2005).

12. S. L. Kadam, K. K. Patankar, C. M. Kanamadi, B. K. Chougule, Electrical Conduction and Magnetoelectric Effect in Ni0.50 Co0.50 Fe2O4 + Ba0.8 Pb0.2TiO3 Composites, *Materials Research Bulletin*, **39**, 2265 (2004).

13. F. Cheng, C. Liao, J. Kuang, Z. Xu, C. Yan, L. Chen, H. Zhao and Z. Liu, Nanostructure Magneto-Optical Thin Films of Rare Earth (RE=Gd,Tb,Dy) Doped Cobalt Spinel by Sol–Gel Synthesis, *Journal of Applied Physics,* **85,** 2782 (1999).

14. N. Rezlescu, E. Rezlescu, C. Pasnicu, M. L. Craus, Effects of the Rare-Earth Ions on Some Properties of a Nickel-Zinc Ferrite, *Journal of Physics: Condensed Matter,* **6**, 5707 (1994).

15. N. Rezlescu, E. Rezlescu, The Influence of Fe Substitutions by R Ions in a NiZn Ferrite, *Solid State Communications*, **88**, 139 (1993).

16. S. Dwevedi, K. K. Bharathi, G. Markandeyulu, Magnetoreactance Studies in Rare Earth-Doped Ni Ferrite, *IEEE Transactions on Magnetics*, **45**, 4253 (2009).

17. M. A. Ahmed, N. Okasha, R. M. Kershi, Influence of Rare-Earth Ions on the Structure and Magnetic Properties of Barium W-type Hexaferrite, *J. Magn. Magn. Mater.,* **320,** 1146 (2008).

18. F. Kools, A. Morel, R. Grossinger, J. M. Le Breton, P. Tenaud, LaCo-Substituted Ferrite Magnets, a New Class of High Grade Ceramic Magnets; Intrinsic and Micro Structural Aspects*, J. Magn. Magn. Mater.*, **242**, 1270 (2002).

19. M. J. Iqbal, M. N. Ashiq, P. H. Gomez, J. M. Munoz, Magnetic, Physical and Electrical Properties of Zr-Ni Substituted Coprecipitated Strontium Hexaferrite Nanoparticles, *Scripta Mater.,* **57**, 1093 (2007).

20. S. B. Narang, I. S. Hudiara, Microwave Dielectric Properties of M-type Barium, Calcium and Strontium Hexaferrite Substituted with Co and Ti ,*J. Ceram. Process. Res*., **7**, 113 (2006).

21. M. J. Iqbal and S. Farooq, Extraordinary Role of Ce-Ni Elements on the Electrical and Dielectric Properties of Sr-Ba M-Type Hexaferrite**,** *Mater. Res. Bull.,***44** 2050 (2009).

22. C. Singh, S. B. Narang, I. S. Hudiara, Y. Bai, F. Tabatabaei, Static Magnetic Properties of Co and Ru Substituted Ba–Sr ferrite, *Mater. Res. Bull*., **43,** 176 (2008).

23. M. J. Iqbal and F. Liaqat, Physical and Electrical Properties of Nanosized Mn, Cr doped Strontium Y-Type Hexagonal Ferrites, *J. Am. Ceram. Soc.,* **93,** 474 (2010).

24. M. N. Ashiq, M. J. Iqbal, M. N. Haq, P. H. Gomez, and A. M. Qureshi, Synthesis, Magnetic and Dielectric Properties of Er-Ni Doped Sr-Hexaferrite Nanomaterials for Applications in High Density Recording Media and Microwave Devices, *J. Magn. Magn. Mater.,* **324,** 15 (2012).

25. G. Asghar and M. Anis-ur-Rehman, Structural, Dielectric and Magnetic Properties of Cr–Zn Doped Strontium Hexa-Ferrites for High Frequency Applications, *J. Alloys Compd*., **526,** 85 (2012).

26. I. Sadiq, I. Ali, E. V. Rebrov, S. Naseem, M. N. Ashiq, and M. U. Rana, Structural, Infrared, Magnetic and Microwave Absorption Properties of Rare Earth Doped Xtype Hexagonal Nanoferrites, *J. Mater. Eng. and Perform.* **7,** 570 (2013).

27. A. B. Gadkari, T. J. Shinde, P. N. Vasambekar , Magnetoreactance Studies in Rare Earth-Doped Ni Ferrite, *Materials Chemistry and Physics,* **114**, 505 (2009).

28. M. T. Farid, I. Ahmad, S. Aman, M. Kanwal, M. Murtaza, I. Ali, I. Ahmad, M. Ishfaq, Structural, Electrical And Dielectric Behavior of $Ni_xCo_{1-x}Nd_yFe_{2-y}O_4$ Nano-Ferrites Synthesized By Sol-Gel Method*, Digest Journal of Nanomaterials and Biostructures,* **10**, 265 (2015).

29. M. Azhar Khan, M. U. Islam, M. Ishaque, I. Z. Rahman, A. Genson, S. Hampshire, Structural and Physical Properties of Ni–Tb–Fe–O System , Materials Characterization, **60**, 73 (2009).

30. N. Rezlescu, E. Rezlescu, C. L. Sava, F. Tudorache, P. D. Popa, Effects of Some Ionic Substitutions on Sintering, Structure and Humidity Sensitivity of MgCu ferrite, *Phys. Stat. Sol. (a).,* **201**, 17 (2004).

31. O. M. Hameda, M. Z. Said, M. M. Barakat, Structural Analysis of Y^{3+}-Doped Mg–Cd Ferrites Prepared by Oxalate Co-Precipitation Method, *J. Magn. Magn. Mater,* **224**, 132 (2001).

32. K. H. Wu, T. H. Ting, M. C. Li and W. D. Ho, Spectral and Transport Phenomena in Ni Ferrite-Substituted Gd_2O_3, *J. Magn. Magn. Mater.,* **298**, 25 (2006).

33. C. W. Kim, J. G. Koh, Sol–Gel Auto-Combustion Synthesis of SiO_2-Doped NiZn Ferrite by Using Various Fuels, *J. Magn. Magn. Mater.,* **257**, 355 (2003).

34. M. S. Hegde, D. Larcher, L. Dupont, Synthesis and Chemical Reactivity of Polyol Prepared Monodisperse Nickel Powders, *Solid State Ion,* **93**, 33 (1997).

35. Ge-Liang Sun, Jian-Bao Li, Jing-Jing Sun and Xiao-Zhan Yang, The Influences of Zn^{2+} and

Some Rare-Earth Ions on the Magnetic Properties of Nickel–Zinc Ferrites, *J. Magn. Magn. Mater.,* **281**, 173 (2004).

36. I. H. Gul, A. Maqsood, Structural, Magnetic and Electrical Properties of Cobalt Ferrites Prepared by the Sol–Gel Route, *Journal of Alloys and Compounds*, **465**, 227 (2008).

37. A. A. Kadam, S. S.Shinde, S. P. Yadav, P. S. Patil and K. Y. Rajpure, Synthesis and Characterization of $CaLaFe_{11}O_{19}$, *J. Magn. Magn. Mater*, **329**, 59 (2013).

38. Ishtiaq Ahmad and Muhammad Tahir Farid, Characterization of Cobalt Based Spinel Ferrites with Small Substitution of Gadolinium, *World Applied Sciences Journal*, **19,** 464 (2012).

39. N. Y. Lanje and D. K. Kulkarni, Synthesis and Characterization of $CaLaFe_{11}O_{19}$, *J. Magn. Magn. Mater.,* 234, 114 (2001).

40. M. N. Ashiq, F. Jahan, M. F Ehsan, M. A. Malana, M. Najam-Ul-Haq and A. M. Qureshi, Effect of Ce-Co Substitution on the Structural, Electrical and Dielectric Properties of Mn Spinel Nanoferrites, *J. Chem. Soc. Pak*., **34**, 1609 (2012).

41. D. S. Birajdar, D. R. Mane, S. S. More, V. B. Kawade, K. M. Jadhav, Structural and Magnetic Properties of $Zn_xCu_{1.4-x}Mn_{0.4}Fe_{1.2}O_4$ Ferrites, *Materials Letters*, **59**, 2981 (2005).

42. L. Nalbandian, A. Delimitis, V. T. Zaspalis, E. A. Deliyanni, D. N. Bakoyannakis, E. N. Peleka, Hydrothermally Prepared Nanocrystalline Mn–Zn Ferrites: Synthesis and Characterization, *J. Micropor. Mesopor. Mater.,* **114,** 465 (2008).

43. M. K. Shobanaa, S. Sankara, V. Rajendranb, Characterization of Co0.5Mn0.5Fe2O4 nanoparticles, *Mater. Chem. Phys.,* **113**, 10 (2009).

44. Rohan Samkaria, Vimal Sharma, Effect of Rare Earth Yttrium Substitution on the Structural, Dielectric and Electrical Properties of Nanosized Nickel Aluminate, *Materials Science and Engineering: B*, **178,** 1410 (2013)**.**

45. T. M. Meaza, S. M. Attiab, A. M. Abo El. Ataa, Effect of Tetravalent Titanium Ions Substitution on the Dielectric Properties of Co–Zn Ferrites, *J. Magn. Magn. Mater.,* **257,** 296 (2003).

46. M. Asif Iqbal, M. U. Islam, Irshad Ali, Muhammad Azhar khan, Imran Sadiq and Ihsan Ali, High Frequency Dielectric Properties of Eu^{+3}-Substituted Li–Mg Ferrites Synthesized by Sol–Gel Auto-Combustion Method, *Journal of Alloys and Compounds*, **586**, 404 (2014)**.**

47. N. Rezlescu, E. Rezlescu, Dielectric Properties of Copper Containing Ferrites, *Physics Status Solidi* A, **23**, 575 (1974).

48. I. H. Gul, A. Maqsood, M. Naeem, M. Naeem Ashiq, Optical, Magnetic and Electrical Investigation of Cobalt Ferrite Nanoparticles Synthesized by Co-Precipitation Route, *Journal of alloys and compounds,* **507**, 201 (2010).

49. M. Kumar, S. Shankar, O. P. Thakur, Anup K. Ghosh, Effects of Co-Substitution on Dielectric, Magnetic Properties and Magnetoelectric Coupling in Nano $CoFe_2O_4$, *Materials Letters***, 143,** 241 (2015).

50. M. T. Farid, I. Ahmad and S. Aman, Characterization of Nickel based Spinel Ferrites with Small Substitution of Praseodymium, *J. Chem. Soc. Pak*., **35**, 793 (2013).

51. M. Raghasudha, D. Ravinder, P. Veerasomaiah, FTIR Studies and Dielectric Properties of Cr Substituted Cobalt Nano Ferrites Synthesized by Citrate-Gel Method, *Nanoscience and Nanotechnology*, **3**, 105 (2013).

52. R. S Devan, B. K. Chougule, Effect of Composition on Coupled Electric, Magnetic, and Dielectric Properties of Two Phase Particulate Magnetoelectric Composite, *Journal of Applied Physics*., **101**, 014109 (2007).